

LOW-PROFILE VERTICALLY POLARIZED OMNIDIRECTIONAL ANTENNAS FOR GROUND SENSOR NETWORKS

Wonbin Hong and Kamal Sarabandi*
University of Michigan
Ann Arbor, MI, 48109-2122

ABSTRACT

This paper presents for the first time low-profile, electrically small antenna with omnidirectional vertically polarized radiation similar to a short monopole antenna. Planar antennas capable of producing vertical polarization have long been sought for many military applications. The paper discusses two distinct and novel techniques that are facilitated to devise antennas that are small as 0.01λ in vertical height and perfectly matched to a 50 ohm source without the need of an external matching network. The antennas are designed, fabricated and measured. Additional studies are performed for further size reductions and performance improvements.

1. INTRODUCTION

Ubiquitous microsensing technology has greatly contributed to the unprecedented control of information and the environment nowadays. Networked microsensors are used for industrial and manufacturing automation, air traffic control, agricultural and environmental screening, etc. In addition, sensor networks have widely been applied to military surveillances such as SOSUS (the Sound Surveillance System), used for the detection of submarines, and AWACS (Airborne Warning and Control System), the air defense system. Susceptibility of evading unwanted detection is vital in many situations, especially in the defense arena. Smart, compact, and easily deployable microsensors are highly desired for applications such as weapon targeting or area denial. Antenna miniaturization is then an important task towards achieving the miniaturization of sensor modules and successful functionality of ground sensor networks. Various types of small antennas with omnidirectional behavior have been studied and proposed [1]-[3]. These methods provide possible means in reducing vertical profiles ($\sim 0.1 \lambda$) while preserving monopole-like radiation behaviors. For many of these antennas, the effect of the ground plane is rather formidable, thus making the horizontal dimension of the antenna electrically large. In this paper, two different approaches to achieve extremely low-profile ($0.01 \lambda - 0.03 \lambda$)

omnidirectional antennas featuring vertical polarization and having small lateral dimensions ($\sim 0.1 \lambda$) are investigated, presented, and discussed. First, a new class of antenna that is derived from the conventional quarter wavelength transmission line resonator is proposed and discussed. The basic structure of the low-profile antenna is composed of microstrip resonators fed by a single probe at a proper location. Quarter-wave elements are shorted to the ground plane and the open-circuited segments are wound around in a spiral-shaped fashion for miniaturization. The overall lateral dimension of the miniaturized multi-element monopole antenna (MMA) is minimized to $0.08 \lambda \times 0.08 \lambda$. The proposed antenna features a vertically polarized omnidirectional radiation behavior while having a vertical height less than 0.03λ . The miniaturized multi-element monopole antenna is further modified to enhance the bandwidth and achieve multi-resonance behavior. The fabricated antennas feature low levels of cross-polarizations, sufficient gains and omnidirectional radiation patterns in the horizontal planes of the antennas.

For conventional monopole antennas, the effect of the ground plane is significant. The effect of the ground plane can be circumvented by shielding the bottom layer of the antenna with a cavity. In addition to the multi-element monopole antenna (MMA), a new technique in designing a cavity-backed omnidirectional antenna with extremely low vertical profile is proposed. The method involves realizing a vertical monopole with a number of folded half-wave slot antennas arranged in a circular geometry to create a miniaturized magnetic loop. Through this method, a novel miniaturized cavity-backed composite slot loop antenna (CBCSLA) with a monopole-like characteristic with less than 0.02λ height is achieved. Additional methods for gain improvements are suggested and presented. The fabricated antenna displays very low input VSWR, low cross polarization and an omnidirectional radiation in the horizontal plane.

Report Documentation Page				Form Approved OMB No. 0704-0188	
Public reporting burden for the collection of information is estimated to average 1 hour per response, including the time for reviewing instructions, searching existing data sources, gathering and maintaining the data needed, and completing and reviewing the collection of information. Send comments regarding this burden estimate or any other aspect of this collection of information, including suggestions for reducing this burden, to Washington Headquarters Services, Directorate for Information Operations and Reports, 1215 Jefferson Davis Highway, Suite 1204, Arlington VA 22202-4302. Respondents should be aware that notwithstanding any other provision of law, no person shall be subject to a penalty for failing to comply with a collection of information if it does not display a currently valid OMB control number.					
1. REPORT DATE 01 DEC 2008		2. REPORT TYPE N/A		3. DATES COVERED -	
4. TITLE AND SUBTITLE Low-Profile Vertically Polarized Omnidirectional Antennas For Ground Sensor Networks				5a. CONTRACT NUMBER	
				5b. GRANT NUMBER	
				5c. PROGRAM ELEMENT NUMBER	
6. AUTHOR(S)				5d. PROJECT NUMBER	
				5e. TASK NUMBER	
				5f. WORK UNIT NUMBER	
7. PERFORMING ORGANIZATION NAME(S) AND ADDRESS(ES) University of Michigan Ann Arbor, MI, 48109-2122				8. PERFORMING ORGANIZATION REPORT NUMBER	
9. SPONSORING/MONITORING AGENCY NAME(S) AND ADDRESS(ES)				10. SPONSOR/MONITOR'S ACRONYM(S)	
				11. SPONSOR/MONITOR'S REPORT NUMBER(S)	
12. DISTRIBUTION/AVAILABILITY STATEMENT Approved for public release, distribution unlimited					
13. SUPPLEMENTARY NOTES See also ADM002187. Proceedings of the Army Science Conference (26th) Held in Orlando, Florida on 1-4 December 2008, The original document contains color images.					
14. ABSTRACT					
15. SUBJECT TERMS					
16. SECURITY CLASSIFICATION OF:			17. LIMITATION OF ABSTRACT UU	18. NUMBER OF PAGES 8	19a. NAME OF RESPONSIBLE PERSON
a. REPORT unclassified	b. ABSTRACT unclassified	c. THIS PAGE unclassified			

2. MINIATURIZED MULTI-ELEMENT MONOPOLE ANTENNA (MMA)

2.1 Antenna Design

The relatively large vertical dimension of a monopole antenna is typically reduced by modifying its geometry to various shapes such as the meander-line or helically loaded monopole as shown in Fig 1. However, there is generally great difficulty in matching these antennas. Radiation powers from short monopole antennas are proportional to the currents induced on them. In practice the level of induced current is limited by the impedance mismatch between the transmission line and the very small radiation resistance of such radiating structures. External matching networks based on lumped elements are lossy which render rather poor radiation efficiency.

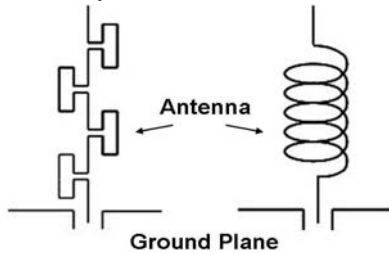


Fig 1. HEIGHT reduced monopole antennas.

One approach to increase the induced electric current on a short segment of a vertical wire above a ground plane is to use the vertical wire as part of a resonant structure. The smallest resonant structure can be formed from a quarter-wavelength segment of a transmission line short-circuited at one end and open-circuited at the other end (i.e. monopole). Consider a microstrip line resonator formed by a strip above the ground plane and short-circuited by a small vertical wire. This resonator can be fed from the center as shown in Fig 2 (a).

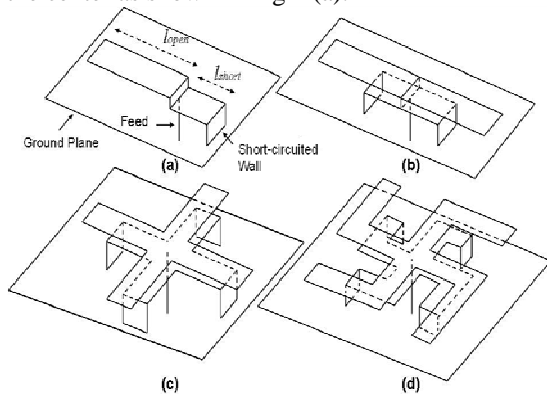


Fig 2. DESIGN process of the MMA.

Impedance matching of this quarter-wavelength resonator (monopole) is facilitated by adjusting the feed position along the resonator and choosing parameters l_{open} the open-circuited segment and l_{short} the short-circuited segment. It is expected that the current flowing on the microstrip itself does not contribute to the total radiated field due to cancellation of the far-field by its image in the ground plane. The directions of the currents at the feed point and on the short-circuited vertical wire are opposite of each other; however, the magnitude of current at the short-circuited wire can be significantly higher from which the net radiation emanates. The electric current flowing on the vertical element of the antenna is responsible for the vertically polarized radiation. If the horizontal electric current can be effectively eliminated we can achieve a completely vertically polarized radiation ignoring the lateral electrical dimension for the time being. Cancellation can be done by adding another monopole element while sharing the same feed as seen in Fig 2 (b). Cancellation of the horizontal electric current is achieved by introducing another set of electric current that is in the opposite direction in the horizontal plane of the antenna with the original electric current at electromagnetic resonance. In contrast, the vertical electric current flowing on the short-circuited pins of each element is in phase and as a result, behaves as the radiating elements of the antenna. Thus, the two-element monopole antenna behaves as a small vertically polarized antenna. To achieve omnidirectional radiation patterns in the horizontal plane of the antenna while maintaining low levels of cross-polarization levels, it is important for the antenna to be electrically small and symmetric. Additional monopole elements are added in similar ways to negate the horizontal currents. The increased number of short-circuited pins provides increased number of radiators and improves the mechanical stability of the multi-element monopole antenna. The topology of the four-element monopole antenna is presented in Fig 2 (c).

The proposed topology of the multi-element monopole antenna enables the height of a traditional monopole antenna to be greatly reduced. However, as the height of the multi-element monopole antenna reduces, the lateral dimension increases. The miniaturization of the multi-element monopole antenna is achieved by folding the open-circuited segments of the antenna in a spiral-shaped geometry so the cancellation of horizontal electric currents on the elements is maintained. To achieve miniaturization, the short-circuited segments of the

antenna can also be meandered and placed slightly below the spiral layer. A sketch of a miniaturized multi-element monopole antenna is visualized in Fig 2 (d). The overall length of each quarter-wavelength segment must be adjusted using a full-wave approach to take the effects of near field mutual couplings into account. The antenna is designed and simulated using Ansoft HFSS and the final topology is shown Fig 3.

As previously mentioned, the input impedance matching of the antenna is achieved by adjusting the length of the open-circuited element and the short-circuited element of the antenna. However, such modification is rather complex, requiring the topology of the antenna to be redesigned and fabricated. Therefore, impedance matching is difficult to achieve through simple tuning of the antenna topology. It has been shown that the length of a slot antenna can significantly be reduced by inserting short-circuited narrow slot-lines along the radiating segment of a slot antenna [4]. Basically, the short-circuited narrow slot-lines behave as series inductive elements. Due to the insertion of series inductive elements, the electric current on the ground plane then transverses a longer path. As result the resonant frequency decreases.

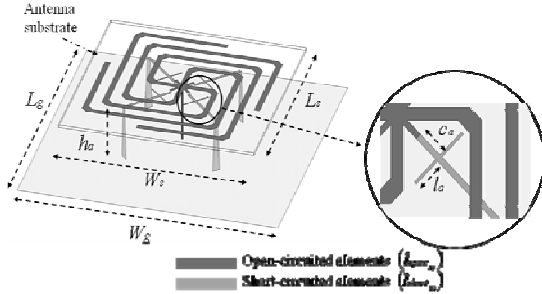


Fig 3. THE finalized multi-element monopole antenna (MMA).

A similar approach is used to modify the short-circuited elements of the miniaturized multi-element monopole antenna. As shown on the right side of Fig 3, a pair of 0.5 mm wide open-circuited microstrip lines are inserted along the short-circuited elements. The insertion of narrow open-circuited microstrip lines introduces shunt capacitance stubs which significantly reduce overall lengths of the short-circuited elements. Impedance matching is obtained by simply adjusting the location ($c_a = 3.5$ mm) and lengths ($l_a = 4.2$ mm) of the inserted narrow microstrip lines. The right angle edges of the spiral-shaped open-circuited elements are replaced with

curved edges. The final lengths of the open-circuited elements l_{open_m} and short-circuited elements l_{short_m} are 144 mm and 20 mm respectively.

2.2 Fabrication and Measurement

The modified antenna is simulated and then fabricated using a $W_s \times L_s = 75 \text{ mm} \times 75 \text{ mm}$ Rogers5880 with thickness of 1 mm, dielectric constant of $\epsilon_{ra} = 2.2$ and loss tangent of 0.0009. The open circuited element and the short circuited element of the antenna geometry are etched on the top and bottom side of the dielectric substrate respectively. The two layers are then connected through via holes. The short-circuited pins are connected to each end of the four short-circuited element. The antenna is fed from the center using a coaxial feed. The antenna height h_a is set to 20 mm. It is a well known fact that the performance of conventional monopole antennas is a function of the ground plane size. Therefore, the integrated antenna structure is first soldered on to a $W_g \times L_g = 50 \text{ mm} \times 50 \text{ mm}$ ground plane and subsequently fabricated and measured on to three other different ground planes with increasing dimensions. The return loss of the fabricated modified multi-element monopole antenna is presented in Fig 4. The antenna displays good impedance matching throughout varying ground plane dimensions.

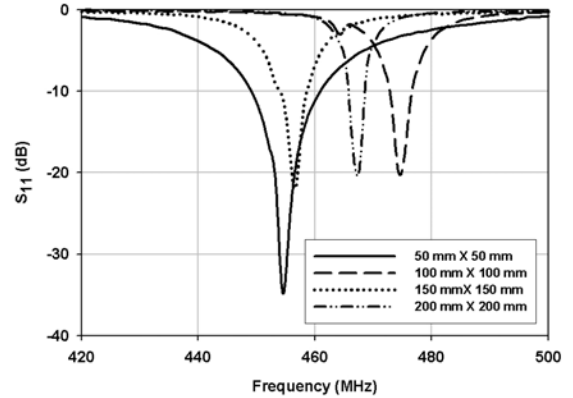


Fig 4. MEASURED S_{11} of the MMA as function of the ground plane.

The shift in resonant frequency can mostly be attributed to the radiating ground plane currents which slightly modify the radiation of the antenna. The far-field co-polarized E-Plane and H-Plane radiation patterns of the antenna are presented in Fig 5. and Fig 6. respectively. As expected when the ground plane dimension is relatively small (0.07λ), the proposed antenna features relatively high cross polarization levels. However, this is

alleviated as the ground plane dimension further increases.

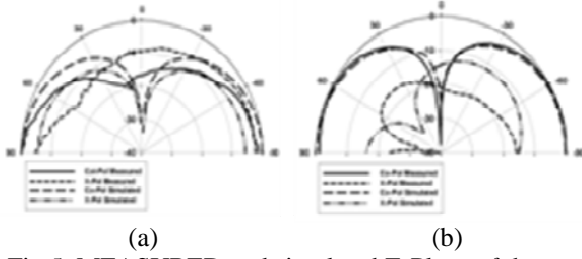


Fig 5. MEASURED and simulated E-Plane of the MMA. (a) $W_g \times L_g = 50 \text{ mm} \times 50 \text{ mm}$
(b) $W_g \times L_g = 200 \text{ mm} \times 200 \text{ mm}$.

The gain of the miniaturized multi-element monopole antenna is measured in the anechoic chamber using a dipole antenna with a known gain.

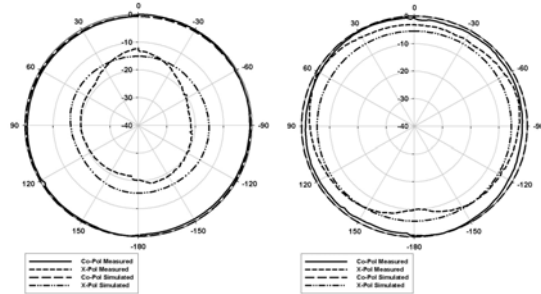


Fig 6. MEASURED and simulated H-Plane of the MMA. (a) $W_g \times L_g = 50 \text{ mm} \times 50 \text{ mm}$
(b) $W_g \times L_g = 200 \text{ mm} \times 200 \text{ mm}$.

The measured 2:1 VSWR bandwidths, gains, and the calculated directivities of the antennas associated with different ground plane sizes are listed in Table I.

Table I. Measured parameters of the MMA as a function of ground plane dimension.

2:1 VSWR (%)	Measured Gain (dBi)	Directivity (dBi)	$W_g \times L_g$ (mm)
3.5	-3.3	1.0	50 × 50
1.6	-1.1	1.1	100 × 100
1.8	0.4	2.0	150 × 150
0.6	1.6	2.8	200 × 200

2.3 The Dual-band MMA

The fundamental resonance of the miniaturized multi-element monopole antenna is determined by the overall length of the antenna arms. The length of the each arm of the antenna is designed to be of identical length to ensure an electrical symmetry of the antenna structure.

Therefore each arm of the antenna features an identical electromagnetic resonance. Adjusting the length of each arm to be of different lengths is found to be ineffective in achieving multi-resonance behavior. Instead, a single resonance which is approximately the average of the combined resonances of each different arm is observed. In addition, transmission zeros limits the multiple resonances from being effectively combined for bandwidth enhancement. Thus, a parasitic coupling approach is used to further improve the bandwidth of the proposed antenna. The dual-band miniaturized multi-element monopole antenna is designed by adding an additional parasitic antenna topology on top of the original modified multi-element monopole antenna structure. Fig 7. shows the geometry of the proposed dual-band multi-element monopole antenna. The driven and parasitic antenna-elements of the proposed antenna are separated by spacing d , which is adjusted by modifying the vertical heights h_p of the short-circuited pins of the parasitic antenna-element. The coaxial feed is connected to the driven antenna-element.

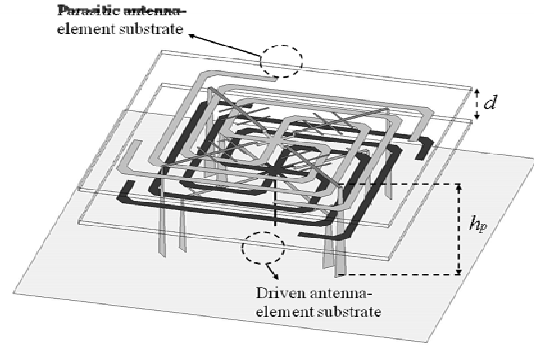


Fig 7. TOPOLOGY of the dual-band MMA.

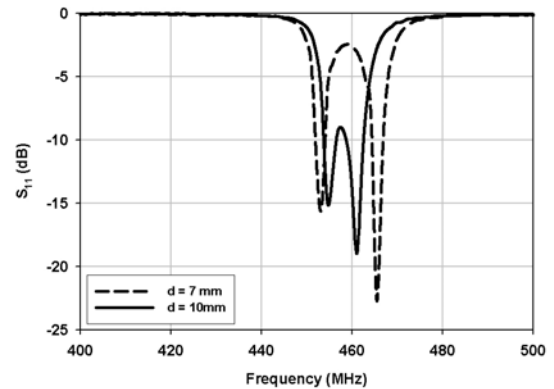


Fig 8. MEASURED S_{11} of the dual-band MMA.

Similar to the original MMA, impedance matching is achieved by adjusting the lengths and locations of the inserted 0.5 mm wide open-circuited

microstrip-lines for each respective antenna-element. The measured return losses of the dual-band MMA are presented in Fig 8. As observed from the figure, by adjusting d , the two resonances of the antenna can be controlled to split or merge with one another.

3. THE CAVITY-BACKED COMPOSITE SLOT LOOP ANTENNA

3.1 Antenna Design

Another approach of devising an electrically small antenna with vertical polarization is investigated in this section. The symmetry of Maxwell's equation can be used to replace a short vertical dipole antenna with a horizontal magnetic loop, which can be realized with a slot loop antenna. However the equivalence relation between a vertical dipole and a slot loop is only valid when the perfectly conducting ground plane is infinitely large. Using field equivalence principle, the slot can be covered with perfect electric conductor with a magnetic current loop above and below. To satisfy the continuity of tangential magnetic field across the slot, the equivalent magnetic currents above and below the PEC have same magnitude but opposite directions. In case of finite size ground plane, cancellation occurs between the radiation of the magnetic loop currents on top of the ground plane and radiation of the magnetic loop current below the ground plane along this plane. That is, there is radiation null along the horizontal plane unlike the radiation pattern of a vertical dipole. Therefore, the ground effect must be shielded in order to alleviate the image cancellation phenomenon and preserve the characteristic behavior of the circular slot antenna.

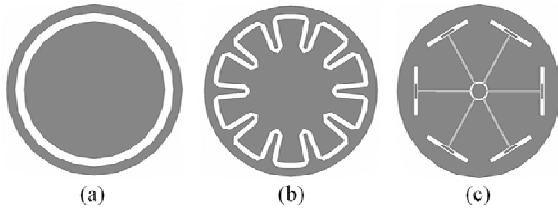


Fig 9. TOPOLOGY of cavity-backed slot loop antennas. (a) Original slot loop. (b) Modified slot loop. (c) Sectionized slot loop for input impedance matching.

It has been found that by implementing a circular slot on the top surface of a metallic cavity, the omnidirectional radiation pattern can be preserved assuming constant current distribution around the

slot can no longer radiate [5]. In addition to achieving omnidirectional behavior, placement of the cavity also preserves the input impedance of the slot antenna, therefore minimizing the sensitivity of the antenna to its surrounding environment.

Despite the implementation of the cavity, there are additional issues that must be addressed to effectively realize the magnetic dipole antenna. First, a constant current distribution around the circular slot must be assured to achieve omnidirectional radiation in the horizontal plane. Fig 9 (a). shows the geometry of a slot loop antenna. However there is much difficulty to match a small cavity backed slot loop antenna to a transmission line. The small slot loop has an open-circuit characteristic and low radiation resistance. To ensure effective radiation off a small loop, significant magnetic current has to be induced in the loop. Without an external matching network, this can only be accomplished if the structure is at an electromagnetic resonance condition. But we are looking for antennas with small electrical dimensions. By modifying the loop in a compact fashion as shown in Fig 9 (b). the dimension can be greatly reduced. However, omnidirectionality and feeding remains problematic. Therefore, to accomplish resonance and achieve sufficient input impedance matching, the magnetic loop can be sectionized into a number of 0.5λ slot antennas around a circle. Fig 9 (c). shows the conceptual geometry of the proposed composite slot loop antenna. Of course this geometry is electrically large and has to be modified, but is shown here to show the feed mechanism. As shown, each slot antenna is capacitively fed with a stub. Such structure eases the difficulty of matching the composite slot loop antenna.

The next step is to miniaturize the geometry of the antenna. It has been shown that the physical dimension of a resonant slot antenna can be reduced significantly by loading a short slot section by inductive loads on the edges [4]. The spiral-like geometry of the inductive slotlines are designed for miniaturization purposes. In this paper, similar technique is applied to design a compact, omnidirectional antenna. The dimension of the proposed six-element cavity-backed composite slot loop antenna(CBCSLA) is reduced significantly. Fig 10. shows the modified geometry of the proposed miniaturized slot loop antenna. In addition to miniaturization, by folding the edges of each slot antenna in a spiral-shape fashion in close proximity to one another, an omnidirectional behavior can be

achieved. Basically, the magnetic currents flowing on the folded edges are negated with the magnetic currents flowing on the edges of the adjacent slot antenna. Therefore the outer rings of the folded slots are left to display a circular current distribution, similar to a slot loop antenna. However, each segment of the antenna is at its fundamental electromagnetic resonance ensuring significant current flow that give rise to high radiation resistance and negligible reactance near the resonance. The antenna is then placed on the top surface of a cylindrical-shaped cavity. The sidewalls and the bottom of the cavity are metalized. This implementation allows the electric currents on the surface of the circular slot antenna to flow along the very short sidewalls of the cavity (less than 0.01λ) creating a radiation behavior similar to that of a vertical wire. This is another physical explanation of how a cavity-backed small magnetic loop antenna radiates vertical polarization in the plane of the antenna.

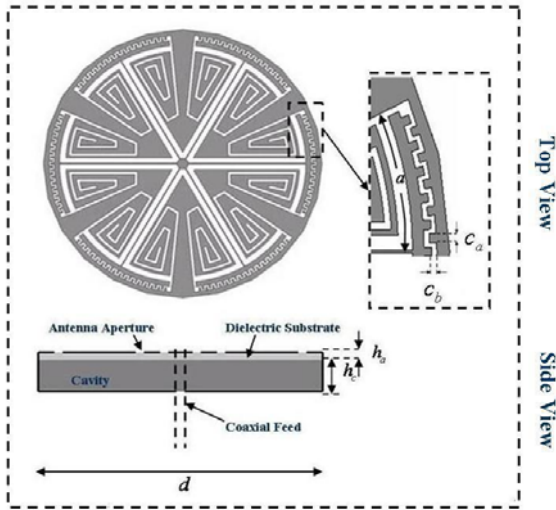


Fig 10. TOPOLOGY of the CBCSLA. The matching network is shown in the right.

3.2 Antenna Feed and Matching

Electrically small antennas often require large impedance transformation matching circuit due to their low resistance and high reactance. When using external matching networks, even while using relatively high Q components, significant loss due to resistance is commonplace. Therefore it is desired to match an electrically small antenna with passive elements while preserving its small dimension. For the miniaturized composite slot loop antenna, a coax feed is used to feed the antenna from the center of

the geometry. The coax feed is connected to six coplanar wave guides (CPW) to feed each of the slots separately. In order to match the six parallel CPW lines to the 50 ohm coax feed, the CPW must be adjusted to 300 ohm. Typically for low dielectric constants, the center conductor of the CPW at high impedance is rather narrow for electrically small antennas, sometimes beyond the fabrication capability. As a result, the width and the gap of the CPW lines were modified to 200 ohm CPW lines. At the edges of each CPW lines, stubs are attached to feed each of the slots capacitively. Miniaturized slot antennas fed at the center near their resonance show relatively high input impedance and therefore it is easier to match them to high impedance transmission lines. As seen from Fig 10, the coupling stubs are corrugated in order to control the capacitance and thus, improve impedance matching to the slot. The impedance matching is adjusted by modifying parameters c_a and c_b in corrugation of the stubs.

3.3 Antenna Simulation and Measurement

The proposed miniaturized cavity-backed slot loop antenna is designed and simulated using method of moments (MoM) based commercial simulation tool (IE3D). The length of the slot line, the width of the CPW lines, and the dimension of the corrugated matching stubs were computed and optimized using full wave simulations. To confirm the intended current distribution and pattern behavior, the magnetic current distribution on the slot-line structure of the antenna is simulated and shown in Fig 11. It is clearly demonstrated that the magnetic currents along the circular arc of individual elements are all following in the same direction with uniform magnitude distribution. Also, the magnetic currents flowing along the spiral arms of adjacent elements are in opposite directions.

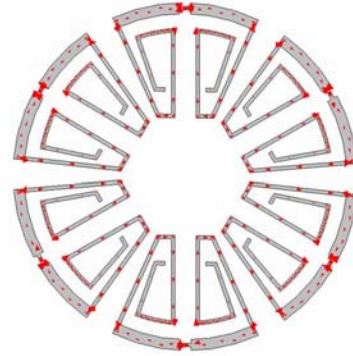


Fig 11. SIMULATED magnetic current distribution of the CBCSLA.

Previous work has shown bandwidth and radiation efficiency of a cavity-backed antenna can be improved by increasing the height of the cavity [6]. To study the effect of the height of the cavity on the slot loop geometry, an additional antenna having identical dimension and topology with a cavity height (h_c) twice as high is designed and simulated. The slot length and corrugations on the matching stub is adjusted to compensate the change of resonant frequency caused by the increase cavity height. The geometrical dimensions and physical parameters of the antennas are presented in Table II. Parameters h_a and h_c are shown in Figure 10.

Table II. Dimensions of CBCSLA (mm)

Antenna height	c_a	c_b	h_a	a	d
$h_c = 6.35$ mm	1.2	0.7	0.5	18.3	100
$h_c = 12.7$ mm	0.6	0.6	0.5	18.3	100

The designed antenna is then built and fabricated on a 0.5 mm thick RO4003 substrate (h_a) from Rogers Corp. The substrate has a dielectric constant of $\epsilon_{ra} = 3.4$ and loss tangent of 0.0027. The fabricated miniaturized slot loop antenna has an overall diameter of 10 cm, less than 0.14λ in electrical dimension. Via holes are drilled along the edges of the antenna platform and wires are soldered. The cylinder-shaped cavity is fabricated by machining a piece of 6.35 mm thick TMM3 substrate (Rogers Corp), which has a dielectric constant of $\epsilon_{rc} = 3.3$ and loss tangent of 0.0020. The bottom of the cylindrical cavity is metalized to create an electrical ground. The fabricated antenna substrate is then placed on top of the cylindrical cavity and the wires are fastened through via holes to the antenna are soldered to the bottom surface of the cavity to electrically connect the antenna to the cavity. Finally, a hole at the center of the cavity-backed antenna is drilled and a coax feed is connected from the bottom of the cavity. The fabrication process is repeated for the antenna with cavity height of 12.7 mm.

The input reflection coefficients of the fabricated antennas are measured using a calibrated HP8720D vector network analyzer and the results are shown in Fig 12. The slight deviation between simulation and measured results is caused by possible errors associated with the numeric simulations, fabrication errors and material tolerances. Both antennas display more than -10 dB reflection coefficients at resonance, indicating good

impedance matching. The far-field co-polarized E-Plane and H-Plane radiation patterns of the antennas are measured in the anechoic chamber at the University of Michigan. The measured E- and H-planes of the antennas with cavity height of 6.35 mm and 12.7 mm are presented in Fig 13, and Fig 14, respectively. Cross-polarization radiations are mostly caused by the close proximity of the feed network cable. Relatively high levels of currents from the electrically small antenna are induced on the nearby cable, causing the currents on the cable to reradiate. This can be confirmed by the change of cross-polarization pattern in Fig 14, as the orientation of the cable connected to the measured antennas are changed. Despite the effect of the feeding network, the measured cross polarization radiations remain significantly lower in the H-plane.

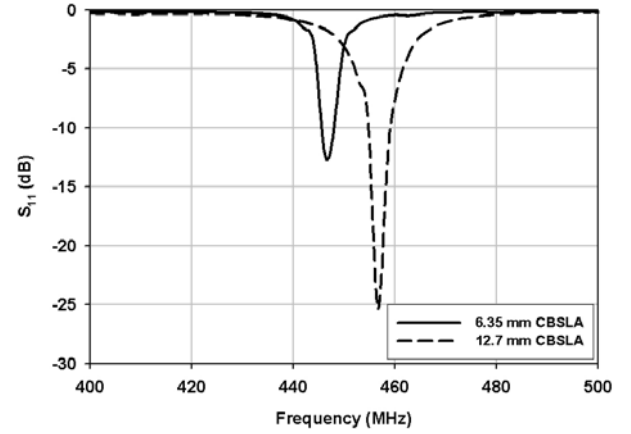


Fig 12. MEASURED S_{11} of the CBCSLA.

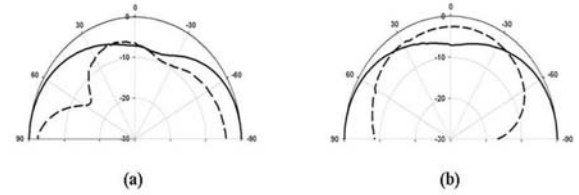


Fig 13. MEASURED E-Plane radiation patterns of the CBCSLA. (a) $h_c = 6.35$ mm. (b) $h_c = 12.7$ mm. Solid Line: Co-Pol. Dash Line: Cross-Line.

The gains of the antennas are measured in the anechoic chamber using a dipole antenna with known gain as a reference and the results are presented in Table III. The directivity of the measured antennas is computed using numerical simulations, and the efficiencies of the antennas are calculated.

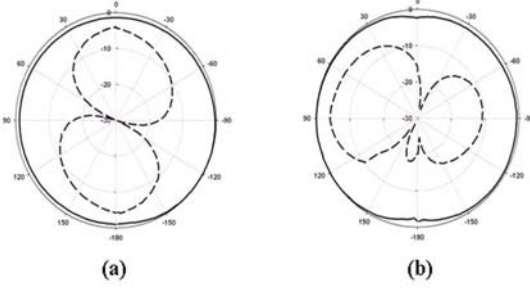


Fig 14. MEASURED H-Plane radiation patterns of the CBCSLA. (a) $h_c = 6.35$ mm. (b) $h_c = 12.7$ mm. Solid Line: Co-Pol. Dash Line: Cross-Line.

It can be observed that by increasing the height of the cavity, the 2:1 VSWR bandwidth is improved and the gain of the antenna increases by 2.2 dB. The improved bandwidth and efficiency remains relatively lower than that of a half wave wire dipole antenna. This can be explained due to the relatively large amount of energy trapped inside the cavity (high Q). As permittivity increases, the fields generated by the antenna tend to be stored within the dielectric material, causing less fields to radiate into the far-field region. However, the measured antenna is much smaller in several orders of magnitude compared to traditional dipole antennas. The bandwidth and efficiency of the cavity-backed miniaturized composite slot loop antenna can be further improved through various methods such as higher quality dielectric, increasing the height of the cavity, or introducing certain boundary conditions such as perfect magnetic conductor (PMC) at the bottom of the cavity.

Table III. Radiation Parameters of the CBCSLA.

Antenna Height	BW (%)	Gain (dBi)	Directivity (dBi)
$h_a = 6.35$ mm	0.7	-3.7	1.6
$h_a = 12.7$ mm	1.1	-1.5	1.6

CONCLUSIONS

A process for designing a new class of miniaturized low profile antennas with vertical polarization is proposed and discussed. The featured multi-element monopole antenna (MMA) displays similar radiation behavior as that of a traditional vertical monopole antenna while having a vertical profile as low as 0.025λ . In addition, a technique for reducing the dimensions of the cavity of a cavity-backed slot antenna is presented, which facilitates

proper fabrication and integration of miniaturized slot antennas on multi-layer substrates. The featured miniaturized cavity-backed composite slot loop antenna (CBCSLA) exhibits excellent matching, omnidirectional radiation patterns in the horizontal plane of the antenna, and moderate efficiency.

ACKNOWLEDGMENTS

This research is supported by the Army Research Laboratory under the Collaborative Technology Alliance (CTA) Micro-Autonomous Science and Technology (MAST).

REFERENCES

- [1] McLean, J., Foltz, H., and Crook, G., 1999: Broadband, robust, low profile monopole incorporating top loading, dielectric loading, and a distributed capacitive feed mechanism, *IEEE International Symposium on Antennas and Propagation*, Vol 3, pp. 1562-1565.
- [2] Hung, K., and Lin, Y., 2006: Open-slot loaded monopole antennas for WLAN and UWB applications, *IEEE International Symposium on Antennas and Propagation*, pp. 4653-4656.
- [3] Yang, F., Aminian, A., and Rahmat-Samii, Y., 2004: A low-profile surface wave antenna equivalent to a vertical monopole antenna, *IEEE International Symposium on Antennas and Propagation*, Vol 2, pp. 1939-1942.
- [4] Behdad, N. and Sarabandi, K., 2004: Bandwidth enhancement and further size reduction of a class of miniaturized slot antennas, *IEEE Transactions on Antennas and Propagation*, Vol. 52, pp. 1928-1935.
- [5] Liao, D. and Sarabandi, K., 2006: Optimization of low-profile antennas for applications in unattended ground sensor networks, *IEEE International Symposium on Antennas and Propagation*, pp. 783-786.
- [6] Hong, W., Behdad, N., Sarabandi, K., 2006: Size reduction of cavity-backed slot antennas, *IEEE Transactions on Antennas and Propagation*, Vol. 54, pp. 1461-1466.